PHOTONICS Research

Active/passive Q-switching operation of 2 μm Tm, Ho:YAP laser with an acousto-optical Q-switch/MoS_2 saturable absorber mirror

Linjun Li,[1,3,*] Xining Yang,[1,4] Long Zhou,[1,4] Wenqiang Xie,[1] Yunlong Wang,[1] Yingjie Shen,[2,8] Yuqiang Yang,[5] Wenlong Yang,[5] Wei Wang,[4] Zhiwei Lv,[3,9] Xiaoming Duan,[6] and Minghua Chen[7]

[1]Heilongjiang Provincial Key Laboratory of Optoelectronics and Laser Technology, Heilongjiang Institute of Technology, Harbin 150050, China
[2]School of Opto-Electronic Information Science and Technology, Yantai University, Yantai 264005, China
[3]School of Electronic and Information Engineering, Hebei University of Technology, Tianjin 300401, China
[4]The Higher Educational Key Laboratory for Measuring & Control Technology and Instrumentations of Heilongjiang Province, Harbin University of Science and Technology, Harbin 150080, China
[5]College of Sciences, Harbin University of Science and Technology, Harbin 150080, China
[6]National Key Laboratory of Tunable Laser Technology, Harbin Institute of Technology, Harbin 150001, China
[7]Key Laboratory of Engineering Dielectric and Applications, Ministry of Education, Harbin University of Science and Technology, Harbin 150080, China
[8]e-mail: Yingjieyj@163.com
[9]e-mail: ZhiweiLV@hebut.edu.cn
*Corresponding author: LLJ7897@126.com

Received 26 February 2018; revised 6 April 2018; accepted 6 April 2018; posted 6 April 2018 (Doc. ID 324784); published 23 May 2018

The active/passive Q-switching operation of a 2 μm a-cut Tm,Ho:YAP laser was experimentally demonstrated with an acousto-optical Q–switch/MoS_2 saturable absorber mirror. The active Q-switch laser was operated for the first time, to the best of our knowledge, with an average output power of 12.3 W and a maximum pulse energy of 10.3 mJ. The passive Q-switch laser was also the first acquired with an average output power of 3.3 W and per pulse energy of 23.31 μJ, and the beam quality factors of $M_x^2 = 1.06$ and $M_y^2 = 1.06$ were measured at the average output power of 2 W.

OCIS codes: (140.3540) Lasers, Q-switched; (140.3580) Lasers, solid-state.

https://doi.org/10.1364/PRJ.6.000614

1. INTRODUCTION

Solid-state lasers with ultra-short pulses operating in the 2 μm wavelength range have been attractive due to their high peak power and pulse energy. Also, they have strong absorption in water and human tissues, and they are in the eye-safe band. So, 2 μm solid-state lasers with ultra-short pulses will be especially promising for applications in medical diagnostics, material processing, surgery, ranging, and nonlinear optical frequency conversion [1–7]. Q-switching techniques are effective methods to achieve ultra-short pulses (nanosecond or microsecond). Among Q-switching techniques, active Q-switching with an acousto-optical (AO) Q-switch is an easy and convenient way to achieve nanosecond (ns) pulse Q-switching operation of a solid-state laser, which can easily get a stable pulse train and tunable pulse repetition frequency as required. The energy of per pulse of the active Q-switched laser can reach millijoule or even joule level. Laser radiation has been demonstrated in the 2-μm waveband, for instance, using a Tm,Ho:YLF crystal, a Tm,Ho:$GdVO_4$ crystal, a Ho:YAG crystal, a Ho:YAP crystal, and a Ho:YLF crystal [8–12].

Different from active Q-switching with extra motivation, passive Q-switching (PQS) with a saturable absorber (SA) is a low-cost and compact way to achieve microsecond (μs) pulse Q-switching operation in the mid-infrared waveband. Due to the limit of the SA's damage threshold, the energy per pulse of the PQS laser achieves only nano or micro joule level, which is lower than the active Q-switching. Many SAs, such as semiconductor saturable absorber mirrors (SESAMs), carbon nanotubes, graphene, black phosphorus, and topological insulators with broadband saturable absorption at 1–3 μm, have been chosen for PQS operations [13–23]. The high damage threshold, ultrafast recovery time, moderate saturation intensity, and broadband saturable absorption from SA have been used as benchmarks against which to judge an excellent SA [24,25]. The SESAMs, as saturated absorbers, were used earlier in the 2-μm waveband, and they have been confirmed in Tm,Ho:YAG, and Tm:LuAG lasers etc. [26–29]. However,

SESAMs have the drawbacks of a complex fabrication process and a narrow operating bandwidth [24]. The graphene as a typically two-dimensional (2D) material with zero-bandgap has been adopted to obtain passive Q-switching operation at the wavelengths of 1, 1.5, and 2 μm [16,28–32], but its weak absorption efficiency at 2 μm limits its modulation ability for light. The carbon nanotubes are typical one-dimensional SA materials that have been widely applied in 1–2 μm fiber lasers [30], but their performance is poor when used in 2 μm solid-state lasers. Black phosphorus is an excellent 2D material owing to its unique structure and properties that make it a promising material for various applications, including SAs [17,18]. However, it is easily oxidized in the presence of oxygen and water, resulting in its poor stability.

Recently, owing to their characteristics of large modulation depth, high nonlinear effects, and broadband saturable absorption, a new type of 2D material, transition metal dichalcogenides [19,20,31–33], have attracted extensive attention. Because of the hexagonal structure of molybdenum atoms sandwiched between two layers of the chalcogen atoms, MoS_2 is an inspiring 2D material representing this class of transition metal dichalcogenides [24,32,33]. The property of thickness dependent electronic band structure largely compensates the weakness of gapless grapheme, which allows it to have some new optical properties and be used in next generation switching and optoelectronic devices [34,35]. To date, few-layer MoS_2 types as SAs have been used in multi-band fiber and solid-state lasers. Zhang *et al.* successfully demonstrated an ytterbium-doped fiber laser with a new type of MoS_2 as an SA in 2014, and the SA was first designed as a MoS_2-taper-fiber device used as a Q-switching SA and a polarization-sensitive optical modulating component [36]. In the same year, Zhang *et al.* proved a MoS_2 mode-locked laser with a pulse duration of 800 ps and a 3-dB spectral bandwidth of 2.7 nm, and the central wavelength of the laser was 1054.3 nm [37]. Tang *et al.* confirmed a passively Q-switched Nd:YVO_4 laser operating at 1064 nm with a few-layer WS_2-SA in 2017, and a pulse duration of 2.3 μs and a single pulse energy of 145 nJ were acquired [31]. Xia *et al.* demonstrated a passively Q-switched Er:YAG laser at 1.6 μm with a YAG-based MoS_2 SA in 2017, and an average output power of 1.08 W with a pulse duration of 1.138 μs and a repetition rate of 46.6 kHz were obtained [38]. Ge *et al.* demonstrated a compact Q-switched 2 μm Tm:$GdVO_4$ laser with a MoS_2 SA in 2015, and 2.08 μJ per pulse energy was achieved at a central wavelength of 1902 nm [20]. However, a 2 μm solid-state laser with an SA being made of MoS_2 in passive Q-switching operations has never been reported with both high beam quality and high average output power.

In this work, we demonstrate the active/passive Q-switching operation of an a-cut Tm,Ho:YAP laser. An active Q-switching operation of a Tm,Ho:YAP laser with an AO Q-switch was pumped by two 794.1 nm laser diodes to generate emissions at 2119.3 nm, and 12.3-W average output power and 10.3 mJ per pulse energy were acquired with 34.2% optical–optical conversion efficiency for the first time. A 3.03 W average output power and 23.31 μJ pulse energy were obtained for the first time from the passive Q-switching operation of a Tm,Ho:YAP laser with an SA mirror of MoS_2, and the beam quality factors of $M_x^2 = 1.06$ and $M_y^2 = 1.06$ were acquired at the average output power of 2 W.

2. EXPERIMENT SETUP

A schematic of the experimental setup is illustrated in Fig. 1: the $^5I_7 \rightarrow {}^5I_8$ laser transition of Ho^{3+} in a Tm,Ho:$YAlO_3$ (Tm,Ho:YAP) crystal was used to achieve a 2 μm wavelength range laser emission. A Tm,Ho:YAP crystal was used in a resonator cavity with a 155-mm physical cavity length. The beam radii in the three mirrors (input, dichroic, and output mirrors) were calculated to be 460, 390, and 320 μm, respectively, by using the ABCD matrix. The beam radii in the laser crystal was calculated to be 420 μm by the ABCD matrix without considering the thermal lens effect, which well matched the pump beam radius of 428 μm. A laser configuration with both ends pumped was used to reduce the thermal loading of the Tm,Ho:YAP crystal. The laser crystals used here were grown at Laser & Optoelectronic Functional Material R&D Center, Shanghai Institute of Optics and Fine Mechanics, China, by the Czochralski technique, the growth direction being along the crystalline c axis for $YAlO_3$ (Pbnm notation), and the laser crystals sample with 5 at. % thulium (1.0×10^{21} ions/cm^3) and 0.3 at. % holmium (0.6×10^{20} ions/cm^3) was cut along its a axis, and the resulting crystal measured to be 4 mm × 4 mm × 8 mm. The end faces of the crystal were coated at both 790–800 nm and 1.9–2.2 μm with a reflectivity of less than 0.5%. One Dewar flask, which was filled with liquid nitrogen, was designed to cool the laser crystal to a temperature of 77 K.

Two laser diodes (LD1 and LD2, nLight Corp. NL-PPS50-10030 and NL-PPS50-10031) with the central output wavelengths of 794.1 nm and 794.0 nm, corresponding to the output powers of 20 W and 20.1 W, were used as the pump source for the Tm,Ho:YAP laser. The temperature of the LD was selected at 298.15 K in the experiment. The output power of each LD was coupled by a fiber with a 400-μm core diameter and a numerical aperture of 0.22, and the central output wavelengths of LD were acquired by adjusting the temperature of the LD.

The pumped lasers from the LDs were refocused on both end faces of the laser crystal by collimation and focus lenses, and the focal lengths of the collimation and focus lenses were 35 mm (collimation lenses) and 75 mm (focus lenses). A pump spot (857.1 μm diameter) was placed at the input surface of the Tm,Ho:YAP crystal. A plane mirror coated with 30% (5%, 7%, 10%, 20%, 25%, 30%, and 35%) transmittance at 1.9–2.2 μm was the output coupler (OC) of the laser.

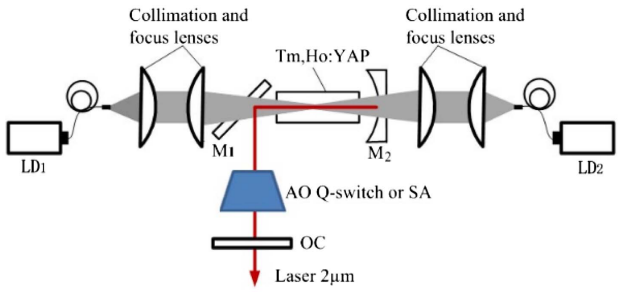

Fig. 1. Schematic of the experimental setup.

A plano-concave mirror (M2) with a radius of curvature of 300 mm, which was coated at 790–798 nm with high transmission ($T > 98.0\%$) coating on both faces, was coated at 1.9–2.2 μm with a high-reflectivity ($R > 99.5\%$) material on its concave face. A flat 45° mirror was used as a dichroic mirror (M1), which was coated at 790–810 nm with high-transmission ($T > 99.0\%$) material and 1.9–2.2 μm with high-reflection ($R > 98.0\%$) material. A fused silica AO Q-switch (QS041-10M-HI7, Gooch & Housego) was used for the active Q-switching experiments with a 46 mm length and a 50 W maximum radio frequency (RF) power; its repetition frequency could be tuned from 1 kHz to 50 kHz. An SA (MoS_2 material) mirror was adopted for the PQS experiments. The mirror made from CaF_2 crystal was used as the substrate of the SA, and a MoS_2 crystal was chosen as the material of the SA. MoS_2 material dissolved in ethyl alcohol was coated onto the surface of one face at the CaF_2 mirror with a spin-coating machine (KW-4A, Chinese Academy of Sciences).

3. RESULTS AND DISCUSSION

Four kinds of OCs (with transmittances of 20%, 25%, 30%, and 35%) were chosen in continuous-wave (CW) mode operation of an a-cut Tm,Ho:YAP laser for optimal transmittance of OC in passive Q-switch mode operation. In CW mode operation, an AO Q-switch was not inserted in the resonator cavity of the Tm,Ho:YAP laser, and the physical cavity length was 155 mm with a pump power of 40.1 W. The output power of the laser was as shown in the insert (upper left-hand corner) of Fig. 2. Under the CW mode operation, the output powers of 13.9, 14.1, 15.6, and 13.3 W were achieved with 20%, 25%, 30%, and 35% transmittance of the OC. As shown in Fig. 2, the transmittance of 30% at 1.9–2.2 μm was the optimal parameter of OC, and stable output power in CW mode operation was acquired with a pump power of 40.1 W. An optical–optical conversion efficiency of 38.9% was obtained, corresponding to a slope efficiency of 40%. So, an OC with the transmittance of 30% at 1.9–2.2 μm was chosen in active Q-switching mode to acquire the stable output performance and match the gain and loss of the laser cavity. When the AO Q-switch was inserted in the 155-mm physical cavity of the Tm,Ho:YAP laser, a 12.6-W output power was acquired in CW mode operation with a pump power of 36.1 W, and an optical–optical conversion efficiency of 34.9%. Compared with the physical cavity without an AO Q-switch, the output power of the Tm,Ho:YAP laser was reduced by 0.7 W due to the insert loss of the AO Q-switch.

The active Q-switching operation is shown in Fig. 2: the average output powers of 12.3, 11.2, 10.8, and 10.3 W were acquired at the pulse repetition frequencies (PRFs) of 10, 5, 2.5, and 1 kHz, and 10.3 mJ per pulse energy was achieved at the PRF of 1 kHz, corresponding to a peak power of 166.7 kW. The power fluctuation at the highest output power was less than 0.3 W within 2 h. The pulse width of the laser in active Q-switching operation is shown in Fig. 3, and the pulse widths of 62.25, 67.2, 65.13, and 61.8 ns were acquired at the PRFs of 10, 5, 2.5, and 1 kHz. The pulse duration at the PRF of 10 kHz was narrower than that of 5 kHz and 2.5 kHz at the maximum pump power because of using a different detector during the measurement. The detector used in the 5 kHz and 2.5 kHz measurements has a longer low-going edge than in the 10 kHz measurement. With a detector (BWPDI-4) and a 320 MHz bandwidth oscilloscope (Tektronix, DPO 3032B), the typical Q-switched pulse train was recorded in 200 ns and 400 ns time scales, as shown in Fig. 4. The peak of similar pulse width in the 400 ns time scale was sharper than that in the 200 ns time scale due to the triggering width of the oscilloscope.

Under the PQS operation, the SA mirror with MoS_2 was inserted into the 155-mm physical length cavity of the Tm, Ho:YAP laser, and it was placed between M1 and the OC. Low transmittances (5%, 7%, and 10%) of the OC at 1.9–2.2 μm were used here to counteract likely output loss, which would otherwise affect the output performance of the laser. The transmittance of the few-layer MoS_2 material at 2119.5 nm was 94.4%, and the modulation depth of MoS_2 material for the laser at 2119.5 nm was 70.6%. Figure 5(a) shows the Raman spectroscopy on MoS_2. The three characteristic peaks of the sample were 384.4, 408.3, and 417.5 cm^{-1}, respectively. Also, the absorption spectrum (which was measured by a

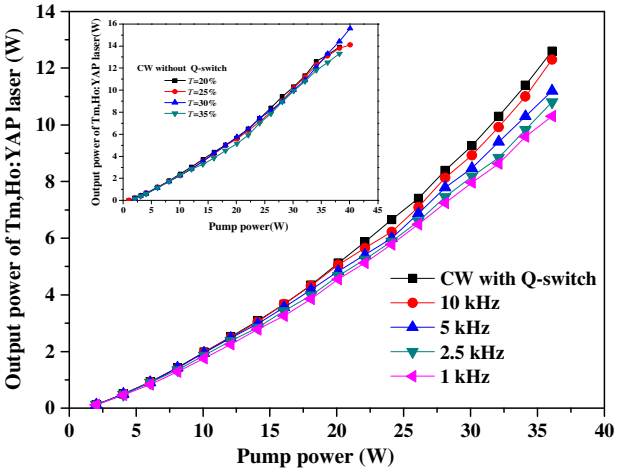

Fig. 2. Output power of the Tm,Ho:YAP laser; the inset is CW output power without Q-switch under different OCs.

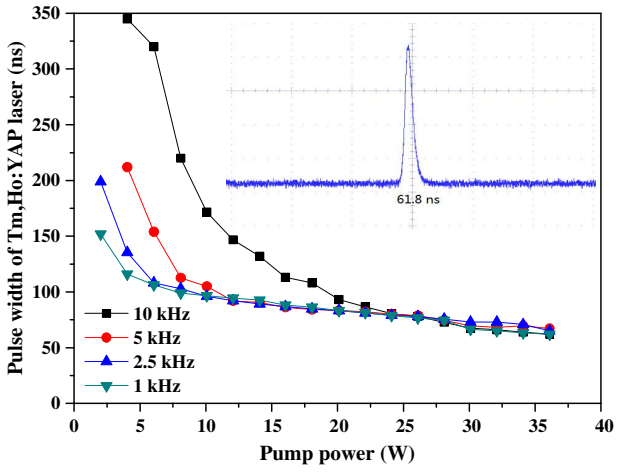

Fig. 3. Pulse width of the Tm,Ho:YAP laser; the inset is typical profile of pulse width in active Q-switch mode.

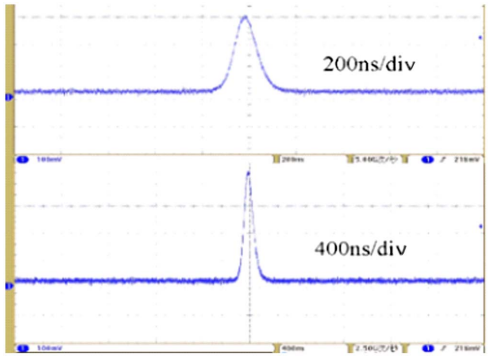

Fig. 4. Pulse train in 200 ns and 400 ns time scales.

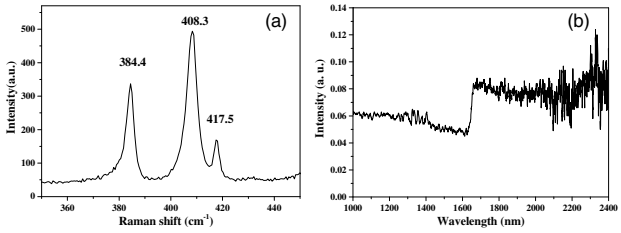

Fig. 5. (a) MoS_2 Raman spectrum; (b) absorption spectrum of MoS_2 material from 1000 nm to 2400 nm.

SolidSpec-3700 DUV UV-VIS-NIR spectrophotometer) of MoS_2 material is shown in Fig. 5, and the absorption intensity of MoS_2 material from 1900 nm to 2200 nm was stronger than the absorption intensity of MoS_2 material from 1000 nm to 1600 nm.

A laser with the output wavelength of 2119.3 nm at 10 kHz in *Q*-switched mode operation was used as the laser source to measure the nonlinear absorption of the material of MoS_2, and the data are shown in Fig. 6. From the nonlinear absorption curve depicted in Fig. 6, the modulation depth, saturation intensity, and initial transmittance were calculated to be 5.1%, 0.091 MW/cm^2, and 87.8%, respectively.

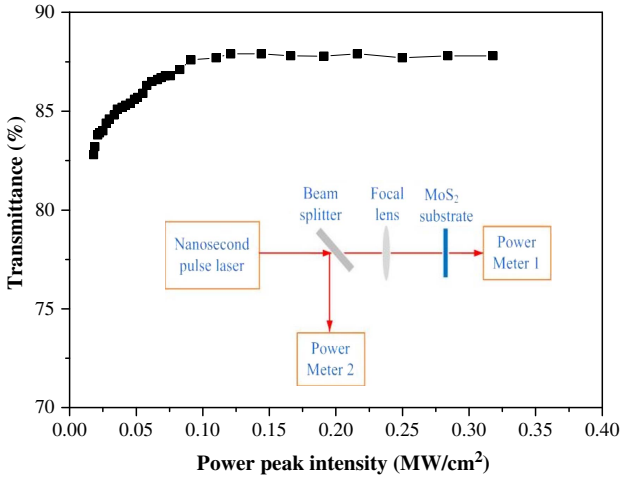

Fig. 6. Nonlinear transmittance curve of the MoS_2 sample versus the pump peak intensities; inset shows the experimental setup for saturable absorption measurement.

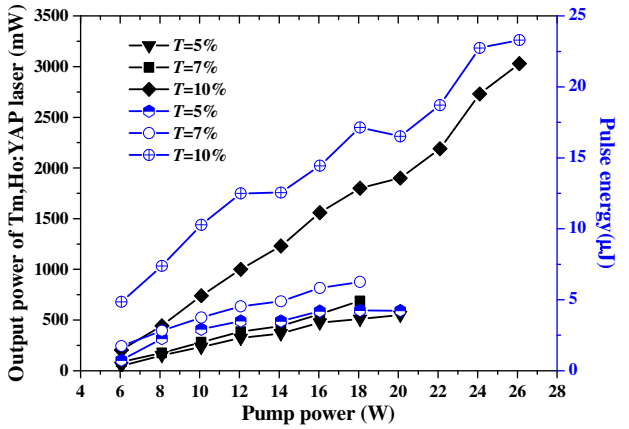

Fig. 7. Output average powers and pulse energies of the Tm,Ho:YAP laser in PQS mode operation.

The output average power and pulse energy of the Tm,Ho:YAP laser in PQS mode operation are shown in Fig. 7: output average powers of 550, 688, and 3300 were acquired with 5%, 7%, and 10% transmittance of OC at 1.9–2.2 μm, corresponding to the pulse energies of 4.23, 6.25, and 23.31 μJ under the pump powers of 20.1, 18.1, and 26.1 W.

The pulse width of the Tm,Ho:YAP laser in PQS operation is shown in Fig. 8. Under the PQS operation with 5%, 7%, and 10% transmittance of OC at 1.9–2.2 μm, the pulse widths of 2.61, 1.64, and 2.37 μs were obtained at the PRFs of 133.6, 110, and 133.2 kHz. The PRFs in three kinds of OCs were increased as the pump power increased, and the pulse widths in three kinds of OCs were reduced. With a detector (Thorlabs, PDA10PT-EC) and a 1 GHz bandwidth oscilloscope (Tektronix, DPO4104), the typical *Q*-switched pulse train was recorded in 4.0 μs and 100 μs time scales, as shown in Fig. 9. The pulse train in the 4.0 μs time scale was not clearer than that in the 100 μs time scale owing to the reason that 3.97 μs pulse width and 87.75 kHz PRF were acquired in the 4.0 μs time scale and 3.20 μs pulse width and 91.2 kHz PRF were achieved in the 100 μs time scale, and the energy value of the former was low. Also, the pulse width

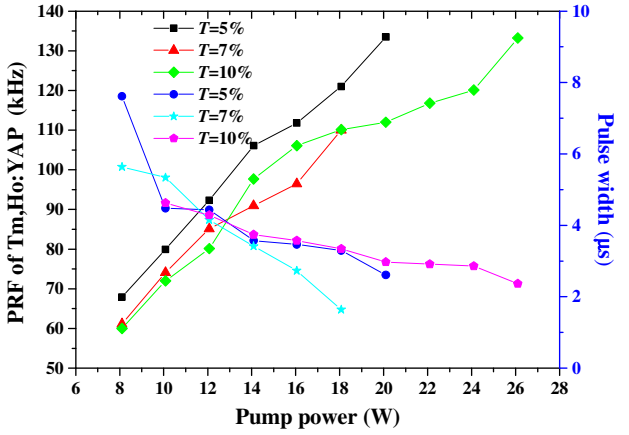

Fig. 8. Pulse width versus pump power and PRF in passive *Q*-switching operation.

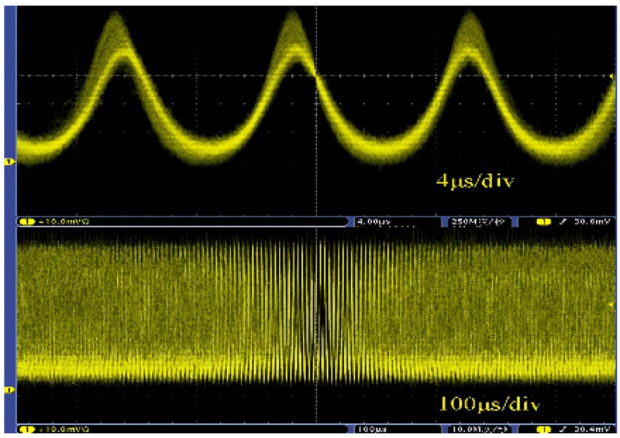

Fig. 9. Pulse train in 4.0 μs and 100 μs time scales.

of the former was near the triggering width of the oscilloscope, and the small burrs in the figure were more. So, the figure of the latter was clear, and pulse width was stable.

A laser wavelength meter (721A IR) with a measurement range of 1.3–5 μm (Bristol Instruments Inc., USA) was used to measure the output wavelength of the Tm,Ho:YAP laser in CW and PQS modes operation, and the output wavelength of the Tm,Ho:YAP laser is shown in Fig. 10. An output wavelength of 2119.5 nm was acquired in CW mode operation, and 2000.4 nm was achieved in PQS mode operation. The central wavelength of PQS was shorter than that of the CW, which was attributed to the stimulated emission cross section in the PQS operation becoming a key factor because the energy stored in the crystal far exceeds the CW operation threshold.

A slit-scanning beam profiler (BP109-IR2) was used to measure the beam quality of the Tm,Ho:YAP laser (Thorlabs Inc., USA), and a two-dimensional laser profile of the output beam from the Tm,Ho:YAP laser was obtained therewith (Fig. 11). Also, the beam quality factors of $M_x^2 = 1.06$ and $M_y^2 = 1.06$ were obtained at approximately 2-W average output power

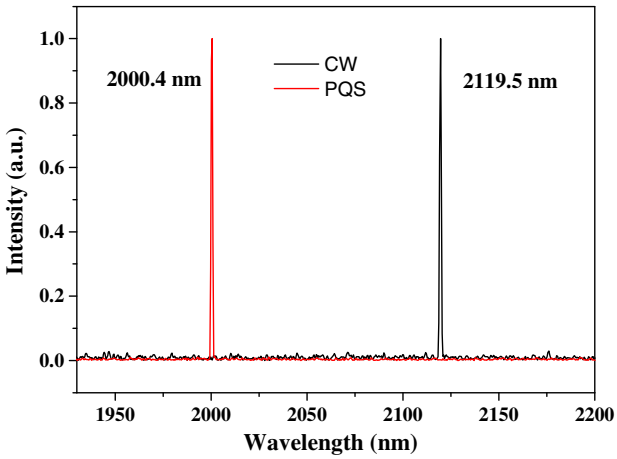

Fig. 10. Output wavelengths of the Tm,Ho:YAP laser in CW and PQS mode operation.

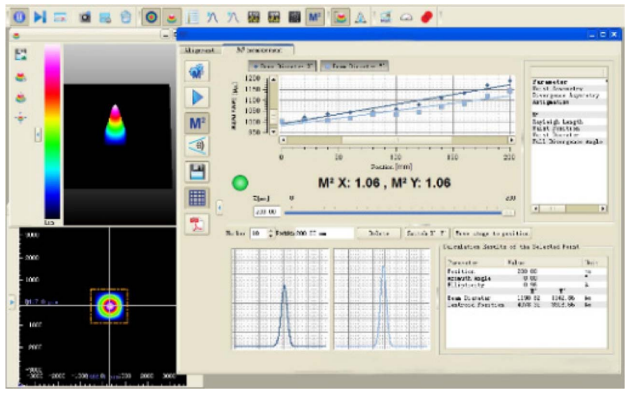

Fig. 11. Beam quality factors of the Tm,Ho:YAP laser.

from the PQS Tm,Ho:YAP laser, corresponding to far-field divergence angles of x:0.048° and y:0.044°.

4. CONCLUSION

In conclusion, we have experimentally demonstrated a high-beam-quality Tm,Ho:YAP laser under active Q-switching and PQS operations for the first time. In the active Q-switching operation, a 12.3 W average output power was achieved with the highest per pulse energy of 10.3 mJ. In the PQS operation, the MoS_2 material was used as the SA, and a 3.3 W average output power and per pulse energy of 23.1 μJ were first acquired. Beam quality factors of $M_x^2 = 1.06$ and $M_y^2 = 1.06$ were achieved at the output power of 2 W.

Funding. National Natural Science Foundation of China (NSFC) (61378029, 61775053, 51572053, 51777046), Science Foundation for Outstanding Youths of Heilongjiang Province (JC2016016), Science Foundation for Youths of Heilongjiang Province (QC2017078).

REFERENCES

1. J. Li, H. Luo, L. Wang, Y. Liu, Z. Yan, K. Zhou, L. Zhang, and S. K. Turistsyn, "Mid-infrared passively switched pulsed dual wavelength Ho^{3+}-doped fluoride fiber laser at 3 μm and 2 μm," Sci. Rep. **5**, 10770 (2015).
2. M. Grasso, "Experience with the holmium laser as an endoscopic lithotrite," Urology **48**, 199–206 (1996).
3. J. Geng and S. Jiang, "Fiber lasers: the 2 μm market heats up," Opt. Photon. News **25**, 34–41 (2014).
4. S. Cha, K. P. Chan, and D. K. Killinger, "Tunable 2.1 μm Ho lidar for simultaneous range-resolved measurements of atmospheric water vapor and aerosol backscatter profiles," Appl. Opt. **30**, 3938–3943 (1991).
5. J. Yu, M. Petros, T. Refaat, K. Reithmaier, R. Remus, U. Singh, W. Johnson, C. Boyer, J. Fay, S. Johnston, and L. Murchison, "Airborne 2-micron double pulsed direct detection ipda lidar for atmospheric CO_2 measurement," EPJ Web Conf. **119**, 03004 (2016).
6. M. Queißer, M. Burton, and L. Fiorani, "Differential absorption lidar for volcanic CO_2 sensing tested in an unstable atmosphere," Opt. Express **23**, 6634–6644 (2015).
7. B. Q. Yao, Y. J. Shen, X. M. Duan, T. Y. Dai, Y. L. Ju, and Y. Z. Wang, "A 41-W $ZnGeP_2$ optical parametric oscillator pumped by a Q-switched Ho:YAG laser," Opt. Lett. **39**, 6589–6592 (2014).

8. X. Zhang, Y. Wang, and Y. Ju, "LD-pumped actively Q-switched Tm, Ho:YLF laser at room temperature," Opt. Laser Technol. **39**, 78–81 (2007).
9. B. Yao, Y. Wang, Y. L. Ju, and W. J. He, "Performance of AO Q-switched Tm, Ho:$GdVO_4$ laser pumped by a 794 nm laser diode," Opt. Express **13**, 5157–5162 (2005).
10. J. Kwiatkowski, J. K. Jabczynski, W. Zendzian, L. Gorajek, and M. Kaskow, "High repetition rate, Q-switched Ho:YAG laser resonantly pumped by a 20 W linearly polarized Tm:fiber laser," Appl. Phys. B **114**, 395–399 (2014).
11. X.-M. Duan, B.-Q. Yao, X.-T. Yang, L.-J. Li, T.-H. Wang, Y.-L. Ju, Y.-Z. Wang, G.-J. Zhao, and Q. Dong, "Room temperature efficient actively Q-switched Ho:YAP laser," Opt. Express **17**, 4427–4432 (2009).
12. J. Kwiatkowski, "Highly efficient high power CW and Q-switched Ho:YLF laser," Opto-Electron. Rev. **23**, 165–171 (2015).
13. D. Nodop, J. Limpert, R. Hohmuth, W. Richter, M. Guina, and A. Tünnermann, "High-pulse-energy passively Q-switched quasi-monolithic microchip lasers operating in the sub-100-ps pulse regime," Opt. Lett. **32**, 2115–2117 (2007).
14. S. Yan, L. Zhang, H. Yu, M. Li, W. Sun, W. Hou, and X. Lin, "Passive Q-switching in a diode-side-pumped Nd:YAG laser at 1.319 μm," Opt. Eng. **52**, 106107 (2013).
15. J. Liu, Y. Wang, Z. Qu, and X. Fan, "2 μm passive Q-switched mode-locked Tm^{3+}:YAP laser with single-walled carbon nanotube absorber," Opt. Laser Technol. **44**, 960–962 (2012).
16. P. A. Loiko, J. M. Serres, X. Mateos, J. Liu, H. Zhang, A. S. Yasukevich, K. V. Yumashev, V. Petrov, U. Griebner, M. Aguiló, and F. Díaz, "Passive Q-switching of Yb bulk lasers by a graphene saturable absorber," Appl. Phys. B **122**, 105 (2016).
17. M. Fan, T. Li, S. Zhao, G. Li, X. Gao, K. Yang, D. Li, and C. Kränkel, "Multilayer black phosphorus as saturable absorber for an Er:Lu_2O_3 laser at 3 μm," Photon. Res. **4**, 181–186 (2016).
18. Y. Xu, W. Wang, Y. Ge, H. Guo, X. Zhang, S. Chen, Y. Deng, Z. Lu, and H. Zhang, "Stabilization of black phosphorous quantum dots in PMMA nanofiber film and broadband nonlinear optics and ultrafast photonics application," Adv. Funct. Mater. **27**, 1702437 (2017).
19. C. Wang, S. Z. Zhao, T. Li, K. J. Yang, C. Luan, X. D. Xu, and J. Xu, "Passively Q-switched Nd:LuAG laser using few-layered MoS_2 as saturable absorber," Opt. Commun. **406**, 249–253 (2018).
20. P. Ge, J. Liu, S. Jiang, Y. Xu, and B. Man, "Compact Q-switched 2 μm Tm:$GdVO_4$ laser with MoS_2 absorber," Photon. Res. **3**, 256–259 (2015).
21. L. Kong, Z. Qin, G. Xie, Z. Guo, H. Zhang, P. Yuan, and L. Qian, "Black phosphorus as broadband saturable absorber for pulsed lasers from 1 μm to 2.7 μm wavelength," Laser Phys. Lett. **13**, 045801 (2016).
22. J. Li, H. Luo, B. Zhai, R. Lu, Z. Guo, H. Zhang, and Y. Liu, "Black phosphorus: a two-dimension saturable absorption material for mid-infrared Q-switched and mode-locked fiber lasers," Sci. Rep. **6**, 30361 (2016).
23. Y. Song, S. Chen, Q. Zhang, L. Li, L. Zhao, H. Zhang, and D. Tang, "Vector soliton fiber laser passively mode locked by few layer black phosphorus-based optical saturable absorber," Opt. Express **24**, 25933–25942 (2016).
24. L. C. Kong, G. Q. Xie, P. Yuan, L. J. Qian, S. X. Wang, H. H. Yu, and H. J. Zhang, "Passive Q-switching and Q-switched mode-locking operations of 2 μm Tm:CLNGG laser with MoS_2 saturable absorber mirror," Photon. Res. **3**, A47–A50 (2015).
25. B. Guo, "2D noncarbon materials-based nonlinear optical devices for ultrafast photonics," Chin. Opt. Lett. **16**, 020004 (2018).
26. K. Yang, D. Heinecke, J. Paajaste, C. Kölbl, T. Dekorsy, S. Suomalainen, and M. Guina, "Mode-locking of 2 μm Tm, Ho:YAG laser with GaInAs and GaSb-based SESAMs," Opt. Express **21**, 4311–4318 (2013).
27. C. Luan, K. Yang, J. Zhao, S. Zhao, T. Li, H. Zhang, J. He, L. Song, T. Dekorsy, M. Guina, and L. Zheng, "Diode-pumped mode-locked Tm:LuAG laser at 2 μm based on GaSb-SESAM," Opt. Lett. **42**, 839–842 (2017).
28. T. Zhao, Y. Wang, H. Chen, and D. Shen, "Graphene passively Q-switched Ho:YAG ceramic laser," Appl. Phys. B **116**, 947–950 (2014).
29. C. Gao, R. Wang, L. Zhu, M. Gao, Q. Wang, Z. Zhang, Z. Wei, J. Lin, and L. Guo, "Resonantly pumped 1.645 μm high repetition rate Er:YAG laser Q-switched by a graphene as a saturable absorber," Opt. Lett. **37**, 632–634 (2012).
30. H. H. Liu, K. K. Chow, S. Yamashita, and S. Y. Set, "Carbon-nanotube-based passively Q-switched fiber laser for high energy pulse generation," Opt. Laser Technol. **45**, 713–716 (2013).
31. C. Y. Tang, P. K. Cheng, L. Tao, H. Long, L. H. Zeng, Q. Wen, and Y. H. Tsang, "Passively Q-switched Nd:YVO_4 laser using WS_2 saturable absorber fabricated by radio frequency magnetron sputtering deposition," J. Lightwave Technol. **35**, 4120–4124 (2017).
32. Q. H. Wang, K. Kalantar-Zadeh, A. Kis, J. N. Coleman, and M. S. Strano, "Electronics and optoelectronics of two-dimensionaltransition metal dichalcogenides," Nat. Nanotechnol. **7**, 699–712 (2012).
33. C. Ataca, H. Şahin, and S. Ciraci, "Stable, single-layer MX_2 transition-metal oxides and dichalcogenides in a honeycomblike structure," J. Phys. Chem. C **116**, 8983–8999 (2012).
34. B. Radisavljevic, A. Radenovic, J. Brivio, V. Giacometti, and A. Kis, "Single-layer MoS_2 transistors," Nat. Nanotechnol. **6**, 147–150 (2011).
35. K. F. Mak, C. Lee, J. Hone, J. Shan, and T. F. Heinz, "Atomically thin MoS_2: a new direct-gap semiconductor," Phys. Rev. Lett. **105**, 136805 (2010).
36. J. Du, Q. Wang, G. Jiang, C. Xu, C. Xiang, Y. Chen, S. Wen, and H. Zhang, "Disulfide (MoS_2) saturable absorber functioned with evanescent field interaction," Sci. Rep. **4**, 6346 (2014).
37. H. Zhang, S. B. Lu, J. Zheng, J. Du, S. C. Wen, D. Y. Tang, and K. P. Loh, "Molybdenum disulfide (MoS_2) as a broadband saturable absorber for ultra-fast photonics," Opt. Express **22**, 7249–7260 (2014).
38. H. Xia, M. Li, T. Li, S. Zhao, G. Li, and K. Yang, "Few-layered MoS_2 as a saturable absorber for a passively Q-switched Er:YAG laser at 1.6 μm," Appl. Opt. **56**, 2766–2770 (2017).